The kinetics and morphology of polyethylene solution crystallization

A. J. McHugh, W. R. Burghardt and D. A. Holland
Department of Chemical Engineering, University of Illinois, Urbana, Illinois 61801, USA
(Received 14 August 1985)

An experimental study has been carried out on the crystallization kinetics and morphology of two high molecular weight polyethylene fractions in 0.1 wt% xylene solutions. Transformation data for the kinetics were taken dilatometrically over a range of temperatures, and Avrami plots for the higher molecular weight fraction ($\bar{M}_w = 3 \times 10^6$) show a change in slope from $n=3$ at low undercoolings to $n=4$ at higher undercoolings. Slopes of 4 resulted for the lower molecular weight fraction (3.8×10^5) over the entire temperature range studied. Analysis of the crystals by optical and electron microscopy and hot stage demonstrated that the growth morphology is three-dimensional and remains the same for both fractions over the temperature ranges used in the dilatometric experiments. Analysis of the transformation data in terms of both the Avrami equation and molecular nucleation and growth models demonstrated that nucleation is heterogeneous, varying between instantaneous and sporadic depending on the molecular weight and undercooling, and adequately described in the latter cases by either three dimensional or monolayer heterogeneous formation. Values for the end surface energies could be conveniently analysed in terms of the Hoffman-type regimes for chain folded crystallization and the discussion suggests that nucleation may be resulting from regions of entangled clusters of the macromolecules.

(Keywords: polyethylene; solutions; crystallization; heterogeneous nucleation; Avrami constants; dilatometry; growth morphology)

INTRODUCTION

The numerous studies which have been carried out on the lamellar crystallization of polyethylene from dilute solution are well documented[1(a-c),2] and can be broadly classified in terms of those which have been concerned primarily with elucidating the morphology of growth and its relationship to crystal properties, and those in which the kinetics and molecular mechanisms of the transformation process have been quantified. Generally speaking for concentrations of the order of 0.1 wt% and less, and molecular weights less than about 5×10^5, the self-seeding method has been the technique of choice since it combines observation of the single crystal morphology with direct measurement of the growth rate of the crystal faces.

Data on the crystallization kinetics have also been obtained over wide ranges of polymer concentration, molecular weight, and solvent type using dilatometric measurement of the overall transformation rate in combination with Avrami-type analyses[3-10]. However, a limitation of these studies has been that the growth morphology of the crystals has not been independently studied. It has generally been assumed that lamellar single crystals were forming[3-6,9,10] even though the conditions differ from those of the self-seeding experiment and, in many cases, an Avrami time exponent results ($n=4$) which is difficult to reconcile with 2-dimensional growth. Also, in a number of instances[6-10], variations in the time exponent (from $n=3$ to $n=4$) have been found, depending on the molecular weight, solvent and undercooling. Since such variations could have been the result of a change in dimensionality of the growth, due to the nature of the Avrami equation[3,11], unique analysis in terms of the nucleation process has not been possible. Although similar limitations have been noted before[1(b),12,13], to our knowledge, this point has not been further pursued in the literature.

In the course of our studies on the flow-induced crystallization behaviour of ultra-high molecular weight (UHMW) polyethylene solutions we have also been concerned with developing an understanding of the quiescent crystallization behaviour using dilatometry. We have observed a change in Avrami exponent similar to the pattern mentioned above and in order to develop an internally consistent explanation we carried out a morphological study of the crystals in conjunction with an analysis of a lower molecular weight fraction. Our purpose in this paper is to present the results of this study since we believe they shed useful light on the nucleation behaviour of UHMW polyethylene solutions as well as offer a basis for a more complete discussion of the kinetic analysis of polyethylene crystallization.

EXPERIMENTAL

Materials

Two samples of linear, high density polyethylene were used. One was an ultra-high molecular weight polymer, UHMW Hercules Type 1900, as obtained, having an intrinsic viscosity of 21 dl/g corresponding to an $\bar{M}_w$ of about 3×10^6 (ref. 14) and an estimated polydispersity index of about 1.82.[15] The second sample was obtained from an initially unfractionated Marlex 6001 ($\bar{M}_w/\bar{M}_n$ as determined by g.p.c. of 5.1) by liquid–liquid phase separation following the technique described elsewhere[17]. Antioxidant-stabilized *p*-xylene was the solvent and butyl cellosolve was used as the precipitant. Fractions were characterized by standard intrinsic viscosity measure-

0032-3861/86/091585-10$03.00

ment in decalin and converted to molecular weights using literature correlations[16,18]. The fraction chosen for study had an intrinsic viscosity of 5 dl/g, corresponding to an $\bar{M}_w$ of 3.8×10^5 and a polydispersity index of about 1.95.

The solvent used in all of our crystallization experiments was a very high purity (spectrophotometric grade) *m*-xylene which was required to avoid reactions at the interface with the mercury fluid of the dilatometer.

PROCEDURE

Dilatometric experiments

Construction and filling of the dilatometers was carried out largely using the technique described by Mandelkern[4]. Polymer concentrations were 0.05 g/55 cc of solvent for the UHMW sample and 0.05 g/50 cc of solvent for the lower molecular weight sample. In the case of the UHMW polymer, in order to avoid pollution of the mercury interface, it was further necessary to purify the sample by recrystallizing six times prior to sealing in the dilatometer. This was accomplished by melting the sample under a nitrogen atmosphere in approximately 30 cc of solvent in an oil bath at 135°C for approximately 15 min, followed by rapid cooling to room temperature to precipitate the polymer. After removal of the supernatant liquid, fresh solvent was added and the procedure repeated a total of 5 times.

Crystallizations were conducted in a stirred, silicon oil bath controlled by a Precision Temperature Controller (Bayley Instrument Co.) which maintained temperature fluctuations less than ± 0.01°C. A cathetometer, calibrated to 0.005 cm, was used to measure the height of the mercury level in the dilatometer and temperature control was such that fluctuations were less than 0.005 cm. Total changes in the mercury height upon completion of the crystallization were about 1 cm for the UHMW polymer and 0.8 cm for the lower fraction. When working with a freshly charged sample of the UHMW polymer in the dilatometer it was found that several crystallization–melting cycles were necessary before complete mixing with the solvent was achieved as noted by the formation of a floc-like precipitate. Then, before transformation experiment, the polymer was dissolved by heating in a separate bath, at about 138°C for a period of 2 h with rigorous, intermittent shaking. We found that, similar to a previous study[8], reproducibility of the isotherms depended on the thermal history; however, with the above procedure, the resulting isotherms were completely reproducible. After dissolution of the polymer, the dilatometer was quickly transferred to the controlled bath set at the desired temperature. The time of transfer was taken as zero time; however, approximately 50 min were needed for the dilatometer to come to complete equilibrium as noted by a constant mercury height. The observed mercury column height at a given time was converted to a fractional transformation in the usual manner[5].

Morphological experiments

For the lower molecular weight fraction, isothermal crystallizations were conveniently carried out in a device similar to that described by Bassett[2,19] which enabled *in-situ* hot filtration prior to removal of the crystal suspensions. In the case of the UHMW polymer, the extremely high viscosity and elasticity of the solutions completely prevented either their *in-situ* filtering or transfer, by pumping or pouring, to a fresh hot solvent environment, though a number of configurations were attempted. Mechanical stirring with fresh solvent was not considered feasible either due to the likelihood of inducing fibrillar growth. The final device used for these samples abandoned the idea of isolating the crystals *in-situ* and consisted of a 20×150 mm side-arm test tube with a ground glass joint at the top for the insertion of a water cooled Leibnitz condenser to prevent solvent loss by evaporation. The tube was fitted with a side arm hose connection to maintain a nitrogen atmosphere.

Crystallizations were carried out following two procedures. In the first, the crystallizer was held isothermally at the temperature of interest for time intervals corresponding to the linear regions of the Avrami plots followed by a rapid quench to 77°C, where it was kept for an additional 80 min to complete the precipitation. It was felt that the sudden change in temperature would cause an easily discernible change in morphology, thus allowing the isothermal growth morphology to be determined. In the second procedure, samples were allowed to crystallize essentially to completion isothermally. Times for the crystal growth (linear region and completion) were taken from the dilatometric data. In order to reproduce the conditions of the dilatometric experiments as closely as possible, solutions were first crystallized under a nitrogen atmosphere a number of times until a finely divided precipitate formed. The solution was then held at 135°C for 2 h before quenching to the crystallization temperature, followed, in the 2 step case, by a further quench at the appropriate time to 77°C. All samples were stored in fresh solvent at room temperature in sealed bottles.

Samples were prepared for viewing under electron microscopy by allowing drops of the crystal suspension to evaporate onto a carbon film substrate followed by mounting on transmission grids in the usual fashion and shadowing with a carbon/platinum mixture.

Small amounts of the crystals were also viewed under white light in the presence of fresh solvent in a standard optical polarizing microscope. Samples were prepared by placing a few droplets of the crystal suspension on a glass slide which was then fitted with a cover slip. Melting point determinations were made with a calibrated Mettler hot stage (FP52) by observing the disappearance of birefringence.

RESULTS

Dilatometric experiments

Figures 1 and 2 show the transformation–time isotherms for each sample plotted on an Avrami basis for the temperature ranges studied. In each case the lowest temperature was fixed by a balance between the induction time and the thermal equilibrium time needed before crystallization could be monitored. The highest temperature was set by the excessively long transformation time. However, the ranges shown are typical of those reported for similar solutions[5,6]. As expected, a linear relation holds over a transformation range from about 4% to about 40% and the intercepts display the large negative temperature coefficient characteristic of a nucleation-controlled process[1(b),5]. At higher transformations, the data display a roughly

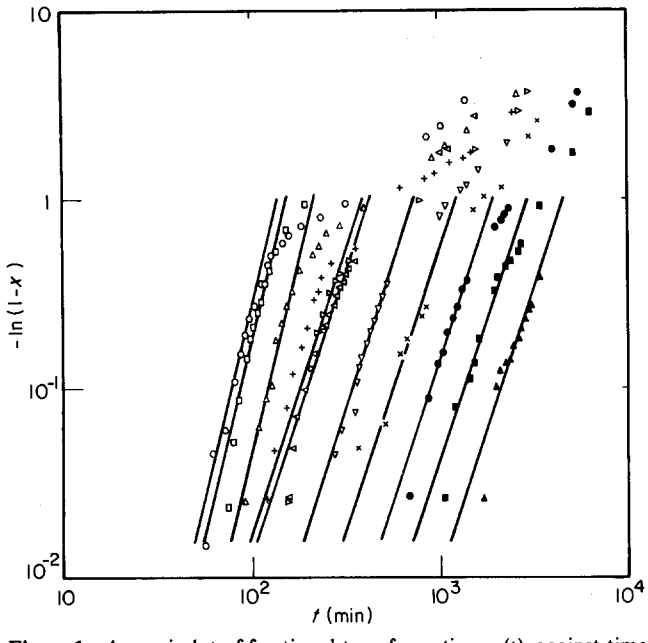

Figure 1 Avrami plot of fractional transformation, $x(t)$, against time for different crystallization temperatures of 0.1 wt% UHMW polyethylene in xylene: (○), 85.45°; (□), 85.8°; (△), 86.2°; (▷), 87.2°; (◁), 87.7°; (▽), 88.5°; (×), 89.15°; (●), 89.98°; (■), 90.5°; (▲), 91°; (+), 86.8°C

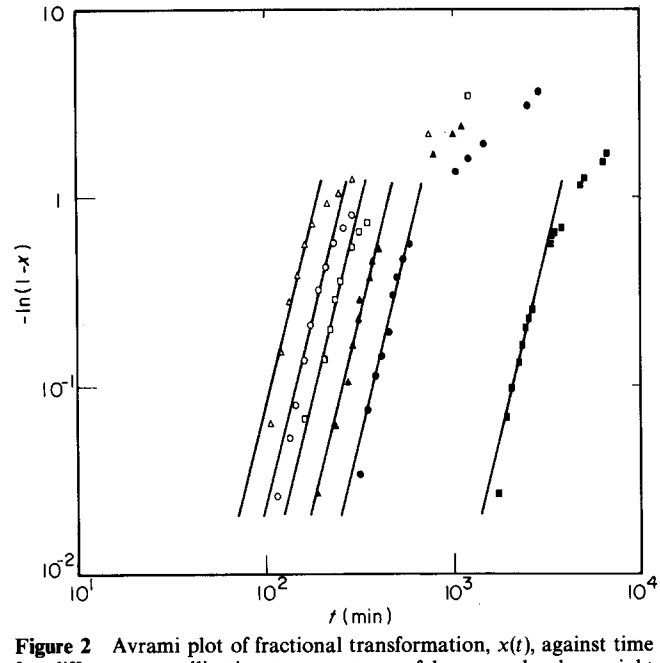

Figure 2 Avrami plot of fractional transformation, $x(t)$, against time for different crystallization temperatures of lower molecular weight polyethylene sample: (△), 86.2°; (○), 86.8°; (□), 87.0°; (▲), 87.5°; (●), 88.0°; (■), 90.0°C

parallel line pattern of reduced slope, similar to the behaviour seen in other studies[8].

The changing slope which occurred for the UHMW polymer shown in *Figure 1* corresponds to a change in the Avrami time exponent, n, from a value of 4 for $T_c = 86.2°C$ and less, to 3 for $T_c = 87.2°C$ and higher. The data taken at $T_c = 86.8°C$ are presented without a line drawn through them; however, they are well fitted by a slope of 3.5. Also data for an isotherm measured at 87.15°C, and fitted by a slope of 3, have been left off the Figure more clearly to show the transitional nature of the slope change. However, the rate constants obtained from those data are included in the analyses given in the next sections.

As shown in *Figure 2*, the transformation behaviour for the lower molecular weight sample exhibited a single Avrami slope of 4 over the entire temperature range studied. One also sees the expected trend of lower crystallization rate as compared to the UHMW sample at similar temperatures. Since interpretation of the kinetic rate constants requires a knowledge of the growth geometry, we present next a discussion of the results of our morphological investigations.

MORPHOLOGICAL CONSIDERATIONS

Bulk morphology

Optical investigations were carried out on crystals of both the UHMW and lower molecular weight samples. In the former case studies were made of the crystals obtained at six of the temperatures corresponding to those studied dilatometrically. These covered the full range from 85.5°C to 91°C and encompassed examples from each of the slope regions. Since *in-situ* solvent rinsing of these crystals was not possible, results will first be presented to establish the growth morphology corresponding to the linear portion of the Avrami transformation plots. In the case of the lower molecular weight solutions both the constancy of the Avrami plot slopes and the ability to carry out *in-situ* hot solvent rinsing of the crystals greatly decreased the number of samples necessary for optical characterization. As will be seen, a principal result was, in fact, the observation that the overall morphology of these crystals is the same as that of the UHMW sample.

Figure 3a shows an optical micrograph typical of the UHMW crystals which, in this case, were crystallized at

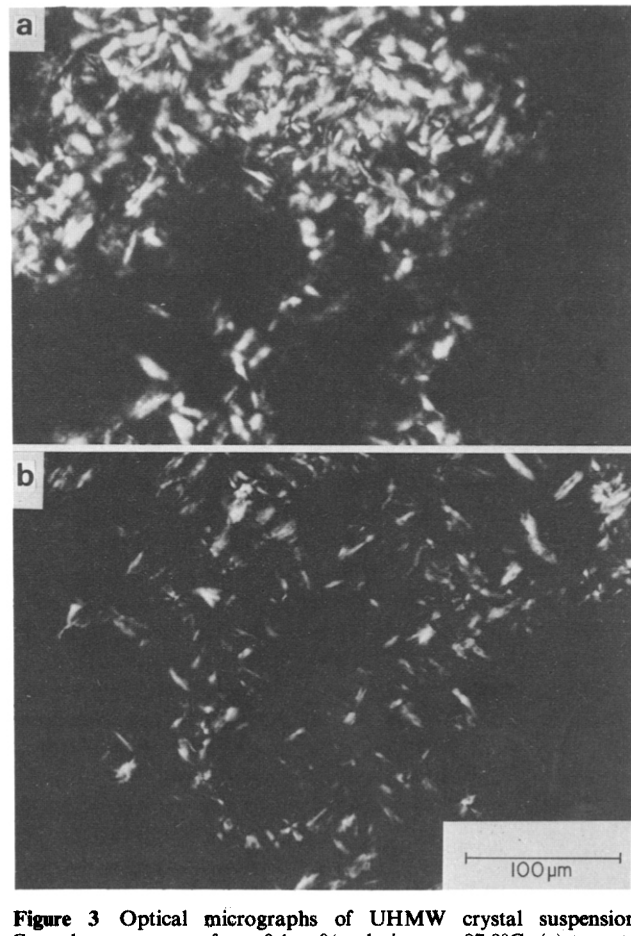

Figure 3 Optical micrographs of UHMW crystal suspensions. Crystals were grown from 0.1 wt% solutions at 87.8°C. (a) two-step growth; (b) single step growth

87.8°C for 300 min followed by quenching to 77°C. *Figure 3b* shows the morphology resulting from single step growth for 3600 min at the same temperature. In both cases samples are being viewed under crossed polars and in the presence of solvent. In *Figure 3a* the crystal growth time corresponds to the linear region of the Avrami plot (*Figure 1*) and the micrograph shows two discinctly different areas: those in which the crystals are relatively large and highly birefringent, similar to the crystals in *Figure 3b*, and those where they are smaller and much less birefringent. In all cases where the 2-step procedure was used such bimodal populations resulted, while none of the samples grown to completion showed the smaller crystals. Furthermore, in all of the 2-step cases, the morphology of the large crystals was found to be the same as that obtained in the corresponding single step crystallization, although slight variations in the crystal sizes were sometimes seen. This result indicates that the larger crystals form at the isothermal crystallization temperature in both cases and that the smaller crystals form upon cooling to 77°C in the 2-step procedure. This conclusion is further corroborated by the pattern observed in the melting point data and shown in *Figure 4*. Here one sees that the samples which were grown in the 2-step procedure always gave two melting points while the isothermally grown samples only exhibited a single melting point. In all of the 2-step samples the small crystals melted at essentially the same temperature, indicating that they all grew at the same temperature, while the crystals grown isothermally, and the large crystals of the 2-step samples, had higher melting points which were also essentially equal. Although, as mentioned, the lower molecular weight suspensions could be rinsed *in-situ*, making the 2-step process unnecessary, a comparison was made of suspensions prepared as above and precisely the same result was found. Thus we conclude that in both cases deviations from the Avrami

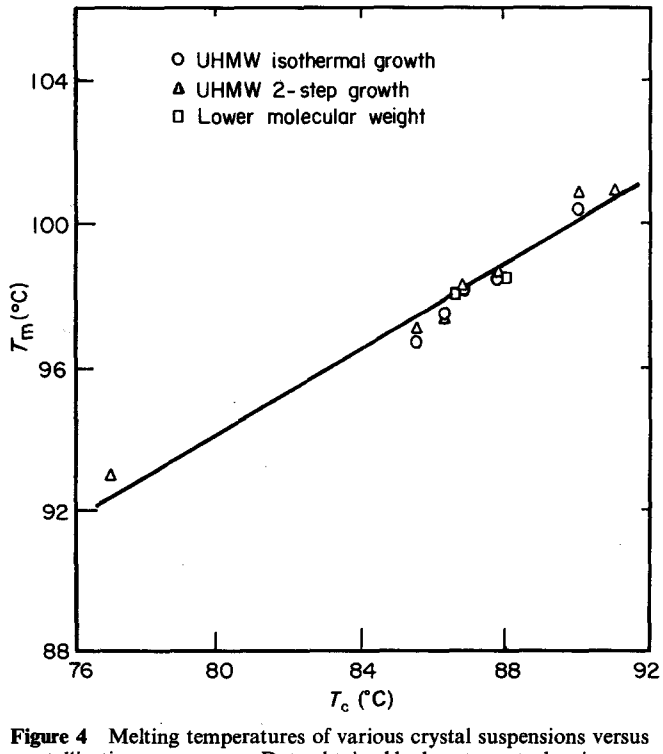

Figure 4 Melting temperatures of various crystal suspensions versus crystallization temperature. Data obtained by hot stage at a heating rate of 10°C/min

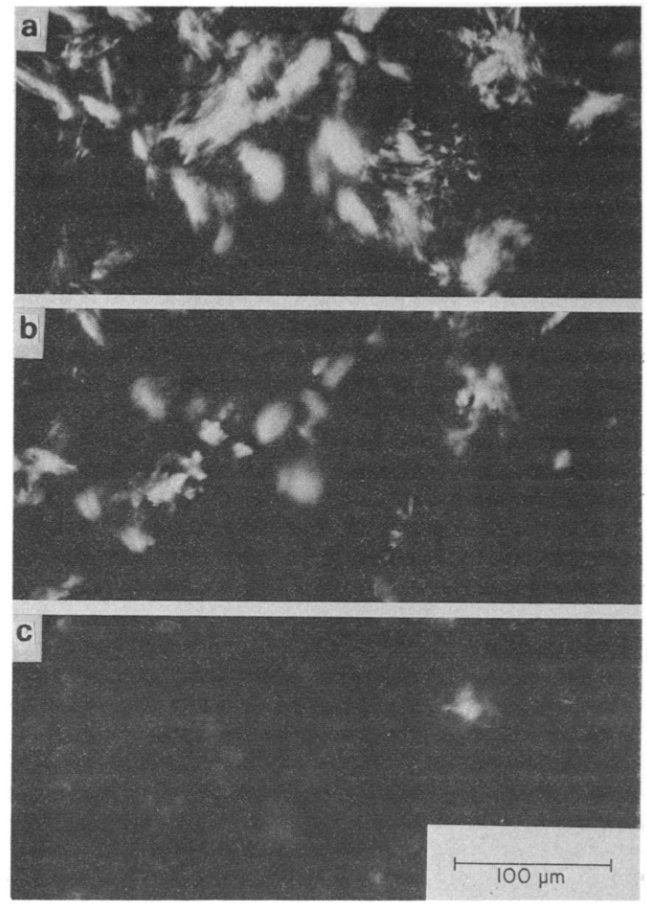

Figure 5 Sequence of optical micrographs showing the effect of solvent evaporation (a)–(c) on UHMW crystals which were grown at 86.2°C

equation at high conversion are neither reflected in nor caused by a change in the growth morphology of the crystals. The logical conclusion in this case is that such deviations are most likely due to the onset of diffusion controlled growth[11,20]. With regard to the UHMW samples, these results also allowed consideration of only isothermally grown crystals for further microscopic observations, thus eliminating complications caused by the presence of the lower temperature population while still ensuring that the observed morphology was the same as that in the linear regime of the Avrami plots. The structures shown in *Figure 3b*, consisting of large elongated crystallites, proved to be the dominant morphology in all of the specimens investigated.

Figure 5 illustrates the effect of solvent evaporation on the crystals of the UHMW sample which, in this case, were grown at 86.2°C. As the solvent evaporates, the crystallites collapse upon themselves with a consequent large decrease in the macroscopic birefringence. The general appearance of these crystallites corresponds strongly to the axialite structures observed in the suspension state at somewhat higher magnifications by Bassett *et al.*[21]. Our electron microscopic observations (to be discussed) also offer further support for the belief that these are highly branched structures, which consist of lamellar layers, supported in a 3-dimensional structure by the surrounding solvent. Presumably, during transformation, the crystallites grow into the solvent in such a way that macroscopic crystalline registry is maintained, therefore leading to the large regions of optical birefringence. Upon evaporation of the solvent the layers

of these crystallites collapse upon one another in a more or less random fashion, destroying the large regions of macroscopic order and thus rendering the original morphology unobservable*.

Figure 6 shows a typical micrograph of the crystallites obtained from the lower molecular weight sample which had been rinsed *in-situ*. One sees a morphology which is similar to that of the high molecular weight sample. In addition, the sequence of events which occurred upon solvent evaporation for these samples was found to be precisely the same as that shown in *Figure 5*. This, together with the melting behaviour (*Figure 4*), indicates that the bulk morphology is indeed the same for both specimens.

The final important observation from optical microscopy is that there appears to be no change in the macroscopic shape of the crystallites formed throughout the temperature range studied in the kinetics experiment. All samples contain the same elongated crystallite structures which appear to consist of a three-dimensional branched lamellar structure supported by solvent.

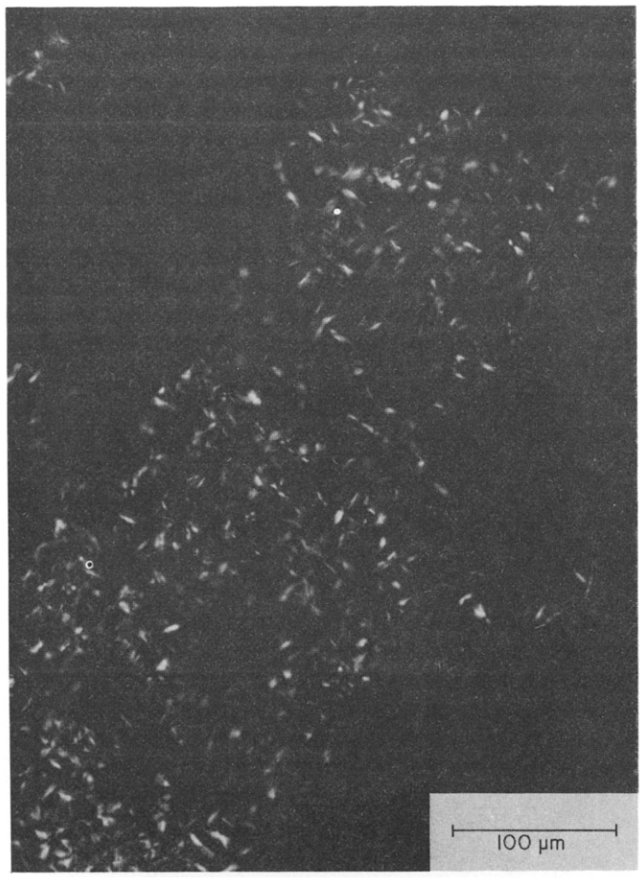

Figure 6 Optical micrograph of lower molecular weight crystal suspension. Crystals were grown at $T_c = 86.8°C$ and rinsed *in-situ*

* We have observed a similar behaviour pattern for polypropylene sheaf/spherulites, grown in solution, which, when suspended in solvent, show the characteristic Maltese cross patterns, but which, when the solvent evaporates, collapse randomly into flat disks which do not exhibit an optical behaviour characteristic of their spherulitic nature. Electron micrographs of these samples also show a loosely branched structure which is lamellar in substructure. We therefore believe that the optical behaviour exhibited by both the polypropylene spherulite structures and the polyethylene crystallites under consideration is caused by the same process, i.e. collapse of an openly branched, three-dimensional structure which had been supported by solvent during growth.

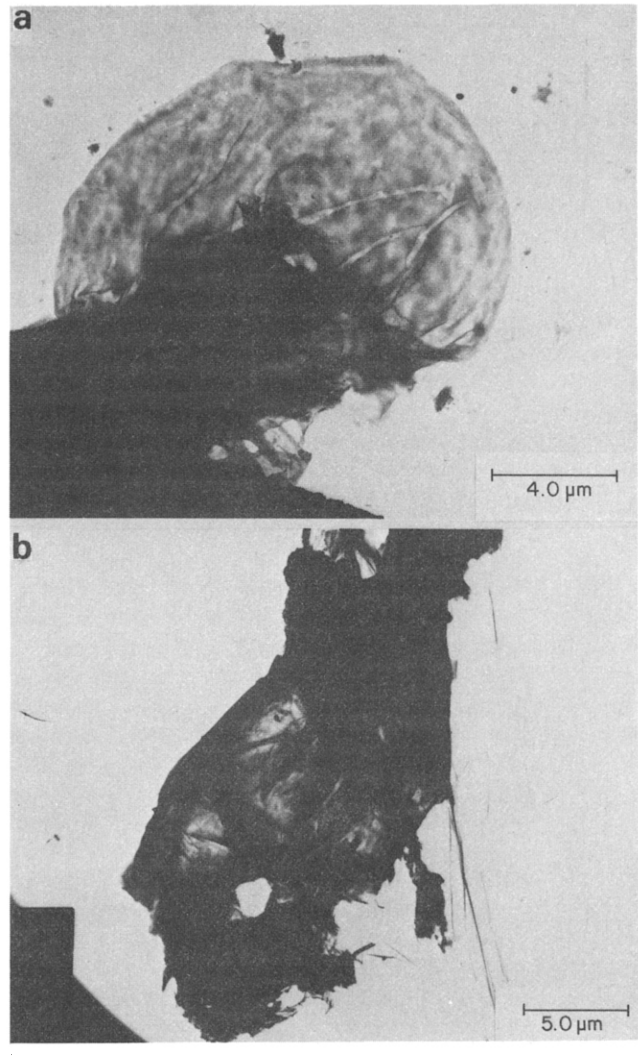

Figure 7 Electron micrographs of UHMW crystals grown at temperatures corresponding to different Avrami slope regions: (a) $T_c = 87.8°C$ ($n = 3$), (b) $T_c = 85.5°C$ ($n = 4$)

Electron microscopy

Investigations of the microstructure were somewhat less unique in that, for a number of samples, different regions of the same specimen exhibited different morphological entities. Since our results from the previous section demonstrated that the morphology of interest remained unchanged in the UHMW samples crystallized to completion, such crystals were examined whenever possible to avoid confusion regarding whether observed structures had formed at the crystallization temperature or during the 2-step quench. Also, since similar results were found for both molecular weight samples, the descriptions which follow will be confined to the UHMW specimens.

Figures 7a and *7b* show typical examples of the primary morphologies observed for the UHMW crystals grown at temperatures corresponding to the two different Avrami slopes. In both cases, the entities shown resemble layered structures of the type observed by Bassett *et al.*[21] in detachment replicas and considered characteristic of collapsed axialites[2,21].

Figures 8a and *8b* show examples, at two different magnification levels, from a different region of the specimen in *Figure 7a* in which an elongated and highly branched lamellar substructure is more clearly apparent.

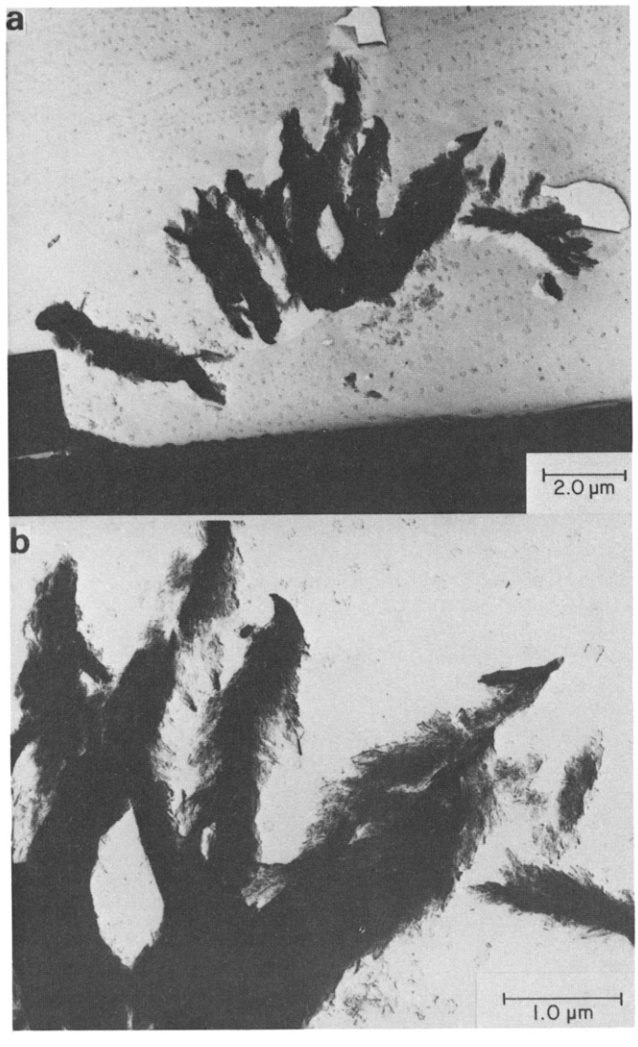

Figure 8 Electron micrographs of separate region of sample shown in *Figure 7a*, showing highly branched lamellar substructure

In both cases we believe that such substructures can be identified with the 3-dimensional, solvent supported structures seen by optical microscopy.

In two of the isothermally grown samples, one of which is shown in *Figure 9*, single crystal lamellae were found to be present. Lamellar thicknesses, determined from shadow lengths, are on the order of 90 Å, which indicates that they formed in the temperature range around 50 to 60°C[22]. Their presence simply indicates that isothermal crystallization had not been quite complete leading to single crystal precipitation from the supernatant solution during the quench to room temperature. On the other hand, this observation shows that the same sample which exhibits lamellar single crystal growth under certain conditions also shows an intricate 3-dimensional development under the conditions dictated by the dilatometric technique. In a similar vein, early studies of single crystals by the self-seeding technique using 0.1 wt% concentrations[23] showed typically large and more complex crystals form upon rapid quenching from high dissolution temperatures to crystallization temperatures on the order of 75°C to 85°C.

Shown also in the micrograph of *Figure 9* are somewhat sphere-like globules (which were observed in a number of other cases) which, unlike the morphologies previously mentioned (*Figures 7* and *8*), have no easily discernible analogue in the optical micrographs. The macroscopic effect of these structures is expected to be low, both due to their small size and the fact that, like the structures in *Figures 7* and *8*, they are three-dimensional in nature and should therefore not affect the Avrami behaviour.

Since the primary purpose of our morphological studies was to establish the general nature and dimensionality of the overall growth morphology, more detailed considerations, of the type described elsewhere[19,21], were not felt to be necessary. We feel our observations are clearly in line with such studies, however, and support the conclusion that crystal growth occurs by a three dimensional process in dilute solutions subjected to the thermal histories used in dilatometry. The resulting structures are clearly not single crystals, appearing instead to be of an axialite or hedrite nature and consisting of a highly branched, 3-dimensional lamellar network which is supported by the solvent during growth. This geometry is the same for both molecular weights and also remains essentially constant for both samples over the full range of crystallization conditions studied. These observations therefore clearly indicate that the variations in slope observed within and between the data of *Figures 1* and *2* are a reflection of changes in the nucleation behaviour and not the growth geometry.

Analysis of transformation kinetics

The dissolution temperature data shown in *Figure 4* are in good qualitative agreement with results reported from several earlier studies[24–29] and can be taken as indicative of lamellar crystallites formed under nucleation-controlled growth conditions[29]. The slope of the straight line fit is 0.6 which compares favourably with several studies[24,29] and the extrapolated value for the

Figure 9 Electron micrograph of single step crystallization sample, $T_c = 86.2$°C, showing single crystal lamellae and sphere-like structures

equilibrium dissolution temperature is $T_s^\circ = 115°C$ which is within the range normally quoted for the polyethylene–xylene system[30]. This value was used in the kinetic analyses to follow.

The Avrami rate constants, k and n, representing, respectively, the intercepts and slopes of the straight lines in *Figures 1* and *2*, can be expressed in terms of the nucleation and growth rates for a three dimensional entity as follows[11,20]

$$kt^n = \left(\frac{\rho_c}{\rho_l}\right) cG^3 \int_0^t (t-\tau)^3 N(\tau) d\tau \qquad (1)$$

In this expression $N(\tau)$ is the nucleation rate per unit volume of solution, ρ_c and ρ_l are, respectively, the crystal and solution densities, G is the linear growth rate, and c is a geometric constant which for the growth of a spherical crystallite would be $4\pi/3$. Equation (1) would also be valid for a 3-dimensional structure characterized by either two or three growth vectors provided that they maintain a constant ratio during growth. In such a case, G would represent a characteristic growth vector with the appropriate proportionality constants absorbed in c. The latter assumption would also be consistent with the constancy we have observed in our growth geometry over the range of temperatures studied.

For the high temperature region in *Figure 1*, the only mechanism which will yield a slope of 3 from equation (1) is that of instantaneous, heterogeneous nucleation which therefore predicts[11,20]

$$k = c' G^3 \bar{N} \qquad (2)$$

where $c' = \left(\frac{\rho_c}{\rho_l}\right) c$ and $\bar{N}$ is the number density of heterogeneities. It is generally well accepted that growth occurs by a 2-dimensional secondary nucleation process which can be formally described by either the fringed micelle or folded chain nucleation models[11,13]. Taking the latter, along with the usual assumption regarding neglect of the activated transport terms, gives[1,2,30]

$$\ln k = \ln(c'\bar{N}) - 3\left(\frac{n' b_0 \sigma \sigma_e}{\Delta H k_B}\right)\frac{T_s^\circ}{T_c \Delta T} \qquad (3)$$

in which ΔH is the crystal heat of fusion, k_B is Boltzmann's constant, T_c is the crystallization temperature, ΔT is the undercooling, σ and σ_e are, respectively, the side and end surface energies of the growth nucleus, and n' is an integer constant whose value is 2 or 4 depending on the assumed growth regime[30]. For cases where no strong transition occurs between growth regimes, an n' value of 3 can result, such as has been reported for polyethylene single crystal growth in xylene[31]. The data shown in *Figure 10* are in good accord with equation (3) (variations in T_s° in the range from 110°C to 118°C had little effect on the linearity seen) and from the slope of the best fit line, using values for ΔH and b_0 given elsewhere[30], lead to a value of 3950 erg^2 cm^{-4} for the quantity, $n'\sigma\sigma_e$. Thus a value of 3 for n' gives the value of 1320 erg^2 cm^{-4} for the surface free energy product, in excellent agreement with previously reported values[30,31] and indicating that a mixture of mechanisms could be contributing to the crystal growth.

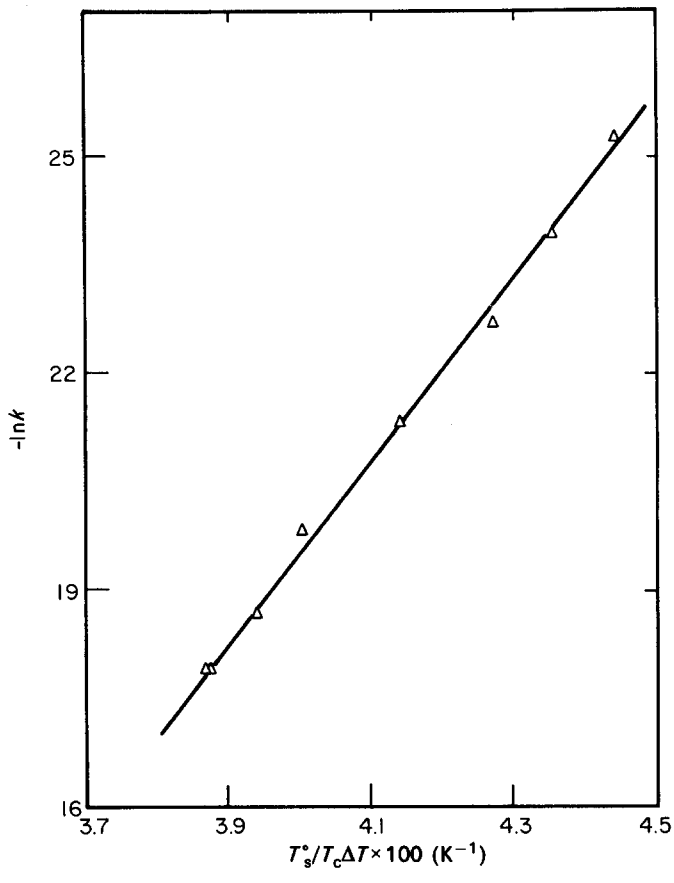

Figure 10 Plot of Avrami rate constant for UHMW polyethylene against $(T_s^\circ/T_c\Delta T)$ for the data in *Figure 1* at lower undercoolings ($n = 3$)

For the three data points at the highest subcoolings resulting in slopes of 4, examination of equation (1) shows that two possible mechanisms could be involved, namely homogeneous nucleation or heterogeneous nucleation at a constant rate (so-called sporadic nucleation)[3,11]. In both of these cases, the temperature dependence of k will contain contributions from both the primary nucleation and growth steps and is given as follows[1(b),13,30]:

$$k \sim \left[\exp\left(\frac{-K_g}{T_c \Delta T}\right)\right]^3 \exp\left[\frac{-32\sigma^2\sigma_e T_s^{\circ 2}}{k_B(\Delta H)^2 T_c(\Delta T)^2}\right] \qquad (4)$$

(homogeneous nucleation)

$$k \sim \left[\exp\left(\frac{-K_g}{T_c \Delta T}\right)\right]^3 \exp\left[\frac{-16\sigma\sigma_e \Delta\sigma T_s^{\circ 2}}{k_B(\Delta H)^2 T_c(\Delta T)^2}\right] \qquad (5)$$

(3-dimensional heterogeneous nucleation)

$$k \sim \left[\exp\left(\frac{-K_g}{T_c \Delta T}\right)\right]^3 \exp\left[\frac{-4b_0\sigma\sigma_e T_s^\circ}{k_B T_c(\Delta H \Delta T - T_s^\circ \Delta\sigma/b_0)}\right] \qquad (6)$$

(heterogeneous, monolayer nucleation)

In these expressions, K_g is given by the collection of constants[30], $n' b_0 \sigma\sigma_e T_s^\circ / \Delta H k_B$, and the quantity $\Delta\sigma$ is the specific interfacial free energy difference accounting for one surface being in contact with the solution and one with the heterogeneous nucleus. In order to test the fit of either equation (4) or equation (5) to the assumed nucleation mechanism, the temperature dependence of

the growth term can be divided out of k using the previously obtained value for the product $n'\sigma\sigma_e$. The latter is consistent with the observed constancy in growth geometry and we believe more rigorous than assuming that the same temperature coefficient will hold for both initiation and growth nucleation as has generally been done[3-11]. *Figure 11* shows that the result of such an analysis leads to a highly non-linear pattern which furthermore, when analysed according to either equation (4) or equation (5), does not yield internally consistent values for the surface energies. Thus the only scheme left is heterogeneous, monolayer nucleation as given by equation (6). If one assumes that $\Delta\sigma$ will be small (which will be proven shortly to be the case for the lower molecular weight fraction) then a plot of $-\ln k$ *versus* $T_s^\circ/T_c\Delta T$ will be linear, as in the case of instantaneous, heterogeneous nucleation, but with a different slope from the latter due to the temperature dependence of the nucleation step. *Figure 12* shows that such is indeed the case, leading to a value of $1470\,\mathrm{erg^2\,cm^{-4}}$ for the $\sigma\sigma_e$ product for $n'=3$.

For the lower molecular weight fraction, since a constant slope of 4 occurred throughout the entire crystallization temperature range, equations (4)–(6) are again applicable. The data are plotted in *Figure 13* according to either of equations (4) or (5) using the same procedure for dividing out the growth rate term from k and show an excellent linear pattern. However, the value for the quantity $\sigma^2\sigma_e$ resulting from the slope of *Figure 13* in conjunction with equation (4) turns out to be $1094\,\mathrm{erg^3\,cm^{-6}}$, a value which is completely inconsistent with the previously reported ranges for $\sigma\sigma_e$ and σ.[30] Analysis of the slope in terms of equation (5), on the other hand, yields $\sigma\sigma_e\Delta\sigma = 2180\,\mathrm{erg^3\,cm^{-6}}$ which, in conjunction with values for $\sigma\sigma_e$ in the range 1200–$1500\,\mathrm{erg^2\,cm^{-4}}$, gives $\Delta\sigma \sim 1$ to $2\,\mathrm{erg\,cm^{-2}}$. To the level of accuracy of our data then we are led to conclude that nucleation could also be characterized as a monolayer, heterogeneous process as given by equation (6) with $\Delta\sigma \to 0$. Accordingly, *Figure 14* shows the excellent linear fit which results; however, a somewhat higher value of

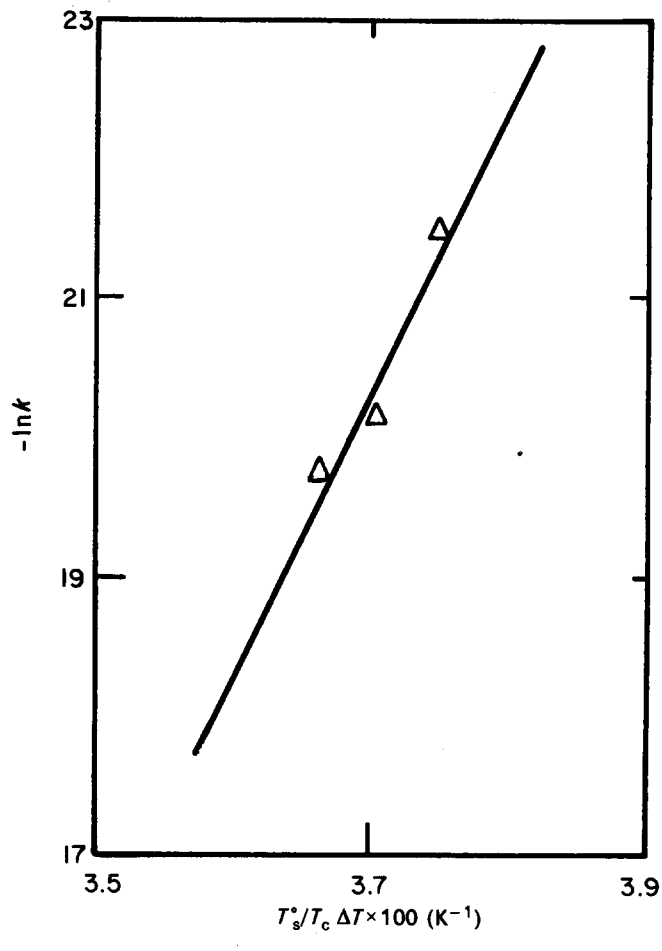

Figure 12 Plot of rate constants from *Figure 11* against $(T_s^\circ/T_c\Delta T)$ according to equation (6) for $\Delta\sigma = 0$

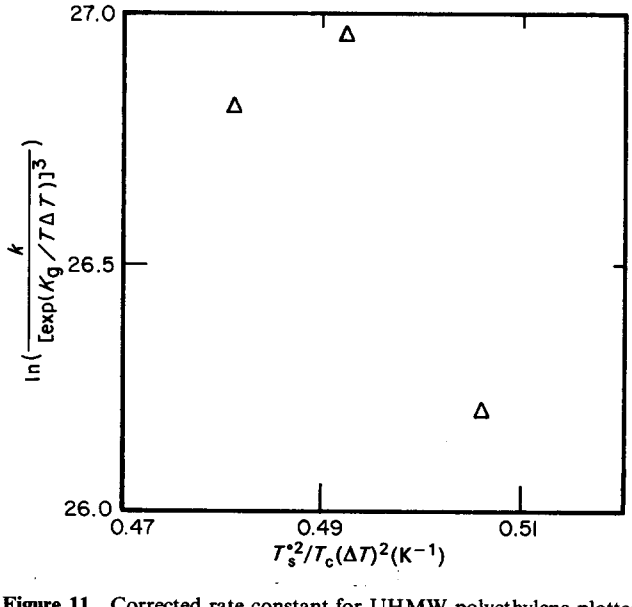

Figure 11 Corrected rate constant for UHMW polyethylene plotted against $T_s^{\circ 2}/T_c(\Delta T)^2$ for the data in *Figure 1* at higher undercoolings ($n=4$)

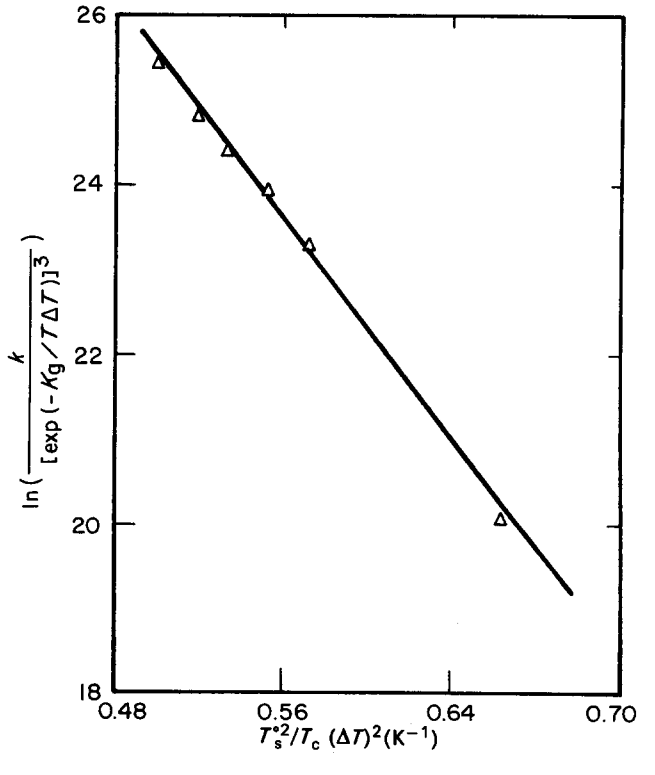

Figure 13 Plot of rate constants obtained from *Figure 2* for lower molecular weight fraction against $(T_s^{\circ 2}/T_c(\Delta T)^2)$

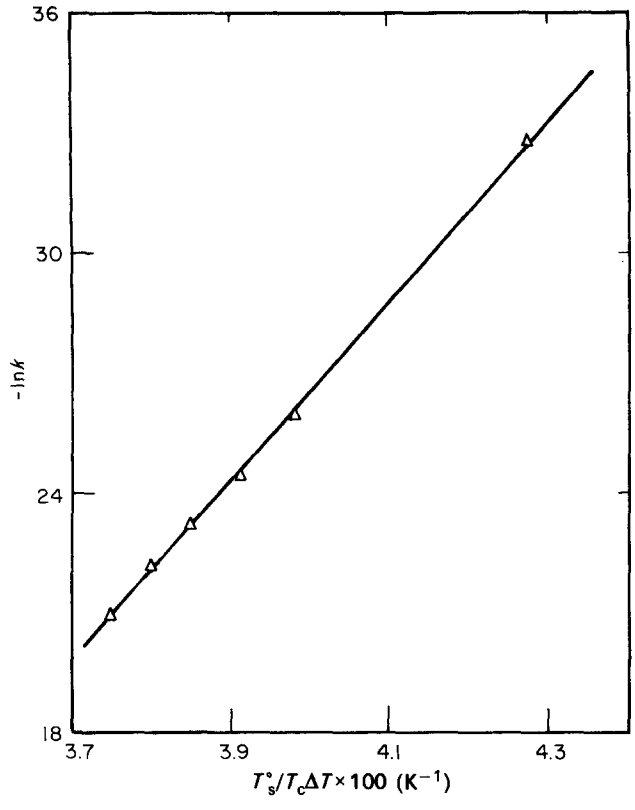

Figure 14 Plot of rate constants from *Figure 13* against $(T_s^\circ/T_c\Delta T)$

5230 $erg^2\,cm^{-4}$ results for the product $n'\sigma\sigma_e$. Hence, in order to obtain a reasonable value for $\sigma\sigma_e$, an n' value of 4, consistent with growth regime I, would be necessary.

DISCUSSION

In several of the dilatometric studies of the polyethylene–xylene system mentioned earlier, concentrations and molecular weights similar to ours were used and values for the Avrami time coefficient were also found to depend on molecular weight[5,6,9]. Coefficients of 3 were reported for an ultra-high molecular weight fraction over the entire temperature range studied[6], while $n=4$ resulted for the lower molecular weights[5,9]. On the other hand, for molecular weights more similar to our lower fraction, variations between coefficients of 3 and 4 have also been observed to occur depending on the solvent type[7-9] (with values of three generally associated with poorer solvents) or undercooling[10]. With regard to the morphology, in all cases, as mentioned, single crystal formation has either been assumed or implied and direct optical verification has not been given, despite the dilemma of having to reconcile slopes of 4 with the two dimensional growth of lamellar single crystals[5,6,9,10]. In fact, reference has been made to studies of bulk crystallization which demonstrated that changes in exponents with molecular weight could not be attributed to any major differences in the basic crystallite morphology[17], an observation which is however fully consistent with our findings. Further, the weight of evidence, especially for polyethylene, indicates that heterogeneous nucleation is the norm and homogeneous nucleation is the rare exception[1(b),13]. On the other hand, the study by Wunderlich and Mehta[32] suggests that a switch from heterogeneous to homogeneous nucleation in solution growth can occur at undercoolings similar to those employed in our study and therefore could be involved. However, as discussed in the kinetic analysis, application of such a scheme to our data (equation (4)) leads to inconsistent results for the nucleus surface free energies for both molecular weights. In addition, the assumption that homogeneous nucleation would also be occurring throughout the entire crystallization range for the lower molecular weight sample seems unlikely, especially given the reduced supercoolings for $T_c > 85°C$.

These observations, together with the internally consistent values obtained for our surface free energies, lead us to conclude that the nucleation mechanism in solution is indeed heterogeneous and displays a varying behaviour pattern which is sporadic or instantaneous depending on the growth temperature and molecular weight (in our case) and possibly also the solvent quality in the previously mentioned studies. A kinetic explanation for a similar behaviour pattern in melt crystallization was suggested by Sharples[33], based on data for spherulitic growth. The basis for this model is the observation that at a given temperature the number of growing sites (nuclei) eventually levels off and that only a fraction of such heterogeneities will be active as the temperature increases. Thus, for a given set of conditions (temperature in this case), either a sporadic or instantaneous nucleation pattern will be exhibited depending on whether the half-life of the overall crystallization process is small or large, respectively, compared with the time to reach the limiting number of active heterogeneities[33]. Price[13] has further suggested that temperature may also affect the level of activity of a given heterogeneity and interactions of the active heterogeneities with the polymer should be weak. Although it cannot be proven from these results alone, it is not unreasonable to speculate that, since our calculated $\Delta\sigma$ values are near zero, segments or clusters of segments of the molecules themselves, perhaps associated with chain entanglements, might be involved as the active sites for crystal nucleation. Since one expects chain entanglement density to increase with increasing molecular weight and decreasing temperature, or solvent quality[34], the observed patterns in Avrami slope values with these variables could be rationalized by such a scheme. Similar considerations might also be involved in the gelation/lamellar crystallization phenomena reported by Edwards and Mandlekern[35] for polyethylene–xylene solutions over a range of concentration, temperature and molecular weight conditions; however, the general validity of such a concept would need to be proven by further studies.

SUMMARY AND CONCLUSIONS

In summary, the following conclusions may be drawn from this study concerning the crystallization behaviour of 0.1 wt% solutions of polyethylene in xylene.

(1) The primary growth morphology, under the conditions used for dilatometric study of the transformation kinetics, consists of elongated, three dimensional lamellar crystallites as opposed to single crystals. This morphology remains unchanged over the entire temperature range studied dilatomatrically and is also the same for the two molecular weights employed.

(2) As a consequence, deviations from linearity in the Avrami transformation behaviour are most likely the

result of diffusion-controlled growth and, more importantly, changes in the Avrami exponent in the linear region from $n=3$ to $n=4$ are the result of changes in the nucleation behaviour from instantaneous to sporadic.

(3) Analyses of the temperature dependence of the Avrami rate constant, k, in terms of chain folded models for heterogeneous nucleation, lead to consistent values for the nucleus surface energies $\sigma\sigma_e$ which can be interpreted in terms of either a mixed Regime I and II mechanism or, for the lower molecular weight, possibly also pure Regime I.

(4) Finally, although the findings are qualitative, it can be reasonably argued that, due to the low $\Delta\sigma$ values found, heterogeneous nucleation may be resulting from clusters or segments of entangled chains. Such a view also lends a qualitative rationale to previous studies in which changes in Avrami coefficient have occurred.

ACKNOWLEDGEMENTS

This work has been supported in part by a grant from the National Science Foundation in cooperation with the Materials Research Laboratory of the University of Illinois, Grant DMR 83-16981.

REFERENCES

1 (a) Wunderlich, B. 'Macromolecular Physics', Academic Press, New York, 1973, vol. 1; (b) *ibid*, 1976, vol. 2; (c) *ibid*, 1980, vol. 3
2 Bassett, D. C. 'Principles of Polymer Morphology', Cambridge Univ. Press, Cambridge, 1981
3 Mandelkern, L. in 'Growth and Perfection of Crystals', (Eds. R. H. Doremus, B. W. Roberts and D. Turnbull), Wiley, New York, 1958, p. 467
4 Mandelkern, L. *Polymer* 1964, **5**, 637
5 Devoy, C., Mandelkern, L. and Bourland, L. *J. Polym. Sci., A-2* 1970, **8**, 869
6 Bourland, L. *Ph.D Thesis*, Florida State Univ., Talahassee, 1973
7 Fatou, J. G., Riande, E. and Garcia Valdecasas, R. *J. Polym. Sci., Polym. Phys. Edn.* 1975, **13**, 2103
8 Riande, E. and Fatou, J. M. G. *Polymer* 1976, **17**, 99
9 Riande, E. and Fatou, J. M. G. *Polymer* 1976, **17**, 795
10 Riande, E. and Fatou, J. G. *Polymer* 1978, **19**, 1295
11 Mandelkern, L. 'Crystallization of Polymers', McGraw-Hill, New York, 1964
12 Hoffman, J. D. and Weeks, J. J. *J. Res. Natl. Bur. Stand.* 1960, **64A**, 73
13 Price, F. P. in 'Nucleation', (Ed. A. C. Zettlemoyer), Dekker, New York, 1969, Ch. 8
14 Technical Information Brochure on 1900 UHMW Polymer, Hercules Inc. Polymers Department 1973 and 'Determination of Intrinsic Viscosity', PTC 179, Hercules Inc. Plastics Technical Center, 1982, p. 6 (Intrinsic viscosity of 1900)
15 Wagner, H. L. and Dillon, J. G. *ACS Div. Polym. Mat. Sci. Eng.* 1984, **50**, 53; and, in 'Polymer Characterization', (Ed. C. D. Craver), Adv. Chem. Ser., 1983, Am. Chem. Soc., Washington, D.C., **203**, Ch. 9
16 de la Costa, M. O. and Billmeyer, F. W. *J. Polym. Sci.* 1963, **A1**, 1721
17 Ergoz, E., Fatou, J. G. and Mandelkern, L. *Macromolecules* 1972, **5**, 147
18 Pal, A. *M. S. Thesis*, Univ. Illinois, Urbana, 1981
19 Bassett, D. C. and Keller, A. *Philos. Mag.* 1962, **7**, 1553
20 Schultz, J. M. 'Polymer Materials Science', Prentice Hall, New Jersey, 1974, Ch. 9
21 Bassett, D. C., Keller, A. and Mitsuhashi, S. *J. Polym. Sci., A* 1963, **1**, 763
22 Miller, R. L. *Kolloid. Z. Z. Polym.* 1968, **225**, 62
23 Blundell, D. J., Keller, A. and Kovacs, A. J. *J. Polym. Sci.* 1966, **B4**, 481
24 Holland, V. F. *J. Appl. Phys.* 1964, **35**, 59
25 Huseby, T. W. and Bair, H. E. *J. Appl. Phys.* 1968, **39**, 4969
26 Blackadder, D. A. and Schleinitz, H. M. *Polymer* 1966, **7**, 603
27 Nakajima, A., Hamada, F., Hayashi, S. and Sumida, T. *Kolloid. Z. Z. Polym.* 1968, **222**, 10; Nakajima, A., Hayashi, S., Korenaga, T. and Sumida, T. *ibid.* 1968, **222**, 124
28 Wunderlich, B., Sullivan, P., Arakawa, T., Dicyan, A. B. and Flood, J. F. *J. Polym. Sci., A-1* 1963, **1**, 3581
29 Jackson, J. F. and Mandelkern, L. *Macromolecules* 1968, **1**, 546
30 Hoffman, J. D., Davis, G. T. and Lauritzen, J. I. in 'Treatise on Solid State Chemistry' (Edn. N. B. Hannay), Plenum Press, New York, 1976, Ch. 7
31 Cooper, M. and St. J. Manley, R. *Macromolecules* 1975, **8**, 219
32 Wunderlich, B. and Mehta, A. *J. Mater Sci.* 1970, **5**, 248
33 Sharples, A. *Polymer* 1962, **3**, 250; Banks, W., Hay, J. N., Sharples, A. and Thomson, G. *ibid.* 1964, **5**, 163
34 Graessley, W. W. *Adv. Polym. Sci.* 1974, **16**, 3
35 Edwards, C. O. and Mandelkern, L. *J. Polym. Sci., Polym. Lett. Edn.* 1982, **20**, 355